coatings

MDPI

Article

Non-Invasive Characterisation of the Wall Paintings in the Byzantine Church of Palazzo Simi (Bari, Italy) and Digital Photogrammetric Survey for a Pigment Mapping

Giovanna Fioretti [1,*], Gioacchino Tempesta [1], Salvatore Capotorto [2] and Giacomo Eramo [1]

[1] Earth and Geoenvironmental Science Department, University of Bari Aldo Moro, 70125 Bari, Italy; gioacchino.tempesta@uniba.it (G.T.); giacomo.eramo@uniba.it (G.E.)
[2] ITC-CNR, 20098 Milano, Italy; salvatore.capotorto@itc.cnr.it
* Correspondence: giovanna.fioretti@uniba.it

Abstract: The paper illustrates the results of a non-invasive characterisation of pigments and their mixtures in the pictorial surfaces of the wall paintings (10th century) found in the Byzantine church of Palazzo Simi in Bari (Italy). The investigation techniques included portable digital polarised microscopy, fibre optic reflectance spectroscopy (FORS) and X-ray fluorescence spectroscopy (XRF). Data comparison supported the recognition of red and yellow ochres, green earth, vine black, minium and Egyptian blue. The presence of some pigment mixtures demonstrated the recurrence of specific technical expedient used by local medieval artists in order to simulate more expensive pigments, which enabled contribution to the understanding of the valuable artistic tradition of the Apulian Middle Age. Both for purposes of conservation and fruition of the site, which is not always accessible, and due to the complexity in taking suitable photographs for the representation of results, the latter was performed on orthophotos extracted from a digital photogrammetric 3D model of the whole archaeological site. By means of chromatic overlapped layers, an interactive compositional map of the pictorial surfaces was produced.

Keywords: pigments; wall painting; XRF; FORS; microscopy; photogrammetry

Citation: Fioretti, G.; Tempesta, G.; Capotorto, S.; Eramo, G. Non-Invasive Characterisation of the Wall Paintings in the Byzantine Church of Palazzo Simi (Bari, Italy) and Digital Photogrammetric Survey for a Pigment Mapping. *Coatings* **2023**, *13*, 996. https://doi.org/10.3390/coatings13060996

Academic Editor: Rodica Mariana Ion

Received: 26 April 2023
Revised: 17 May 2023
Accepted: 24 May 2023
Published: 26 May 2023

1. Introduction

In the last 20 years, Apulian medieval and Renaissance wall paintings, studied widely and in-depth, both from an historical and artistic point of view, have been the subject of a thorough campaign of archaeometric and diagnostic investigation. This has produced interesting results on pictorial techniques, the *modus operandi* of local artists and raw materials, in terms of mortars, plasters, binders and pigments.

Research findings have revealed a chromatic palette composed mainly of natural mineral pigments, including ochres and earths, and organic blacks [1,2], in addition to less common pigments, among which are malachite, azurite, verdigris, massicot, minium, and even cinnabar and lapis lazuli [3–9].

In addition to what is generally observed in the wall painting tradition, the skilful ability of the local artists to blend two or more common and inexpensive pigments to create several hues and shades, especially to replace more expensive and rarer pigments, was highlighted. Examples of this creative expediency are extremely widespread in the region. Noteworthy is the use of carbon black mixed with small amounts of yellow and red ochre to replace more expensive blue pigments for the mantle of the Virgin Mary, the foremost figure in medieval painting [8].

Similarly interesting is a rather complex mixture mainly made up of red ochre, to which minium, cinnabar and realgar were added [4]. Another recipe found was based on the addition of verdigris and malachite to the green earth [4].

The colour rendering of pigments and mixtures was certainly influenced by other factors, including the quality and purity of the raw materials, the binder used as a dispersion medium and the grain size. However, no noticeable differences were observed in the regional wall paintings created via the use of frescos or lime painting techniques. The latter generally differ in the manner of depiction and in the thickness of the pictorial layer. In the frescos, the pigment is dissolved in water and applied to the still-wet plaster, creating a thin layer; instead, in the lime painting, the pigment is mixed with lime milk and painted on the dry plaster surface, creating a thicker layer than the previous case [10].

The need for and effectiveness of non-invasive approaches for the study of wall paintings and their constituting materials is widely reported in the literature and the choice of sustainable and low-impact strategies for the conservation of cultural heritage is now established. In addition, traditional, non-invasive investigation techniques, such as XRF [11–17], are becoming increasingly portable and effective, thanks to ever-growing databases. At the same time, other less consolidated techniques, such as FORS [4,18–24], are advancing in the characterisation of pigment.

Furthermore, recent studies have also highlighted the usefulness of portable digital microscopy both for a preliminary observation of pictorial surfaces and for morphological and dimensional characterisation of pigment particles for identification purposes [24–27].

A further challenge to improve the quality of the research and results from the investigations on pictorial surfaces is the introduction of digital technologies for their representation, visualisation and even sharing.

New digital technologies are currently involved in the field of cultural heritage, both for conservation and research purposes [28–30], and are proving to be efficient and appropriate to produce satisfactory results.

Among them, digital photogrammetry is a cheap and versatile reconstruction technique, and has had positive implications in the study and digital representation of any type of cultural heritage, i.e., archaeological [31,32] and inaccessible sites [33–38], underwater ruins [35] and small artefacts [39,40]. Moreover, in the field of scientific research, the digital products obtained can be useful not only for the virtual representation of an artwork but also in documentation [41], monitoring [42], in the analysis of states of degradation [43,44] and for material mapping [45–49].

This paper combines the results of the investigation carried out on the surface pictorial layers of the wall painting in the archaeological site of Palazzo Simi (Bari, Italy), based on a fully non-invasive, multi-analytic approach. The comparison of the observations under the portable polarised optical microscope, reflectance features obtained by FORS (fiber optic reflectance spectroscopy) and the chemical composition inferred by XRF analysis, has enabled the identification of the pictorial surface pigments.

Furthermore, the use of digital photogrammetry for the creation of a high-resolution 3D model was fundamental to depict the analytical data on specific orthophotos, free of aberrations or optical defects deriving from traditional photography used in very small spaces, and graphical errors due to the curved morphology of the painted surface.

Among the research aims, the most important is definitely the achievement of a cognitive framework on the materials used in the wall painting, in order to contribute to the reconstruction of its history and events, including previous retouching and restoration actions. These objectives also help in augmenting current knowledge on the pictorial materials used in the Apulian painting. On the other hand, thanks to the use of digital technologies, the paper aims to produce a digital survey for conservation and research purposes, as it can be remotely consulted, and to represent the data on a map, thereby introducing a more interactive and immediate approach to depicting the results.

Archaeological and Artistic Context

The studied wall painting is located in the church under the Palazzo Simi, currently the headquarters of the Authority for Archaeology, Fine Arts and Landscape for the metropolitan city of Bari, Italian Ministry of Culture. It is one of about 10 Byzantine

churches discovered during the archaeological excavations carried out over time, and is bonded with the masonry built in later periods [50,51].

Not much information is known about the archaeological site, and even the saint to whom it was dedicated is unknown, although some archival sources have suggested a connection with St. Gregorio. The discovery of two coins—issued during the reigns of emperors Constantine II and (his wife) Zoe, and emperor Giovanni Zimisce, respectively [52]—proved that the church and the paintings can be dated to the 10th century.

The lowest part of the three apses of this small church with a Greek cross plan (about 10–11 m × 6 m), exhibiting the studied wall painting fragments, has been preserved. The wall painting depicts the lower part of four Byzantine bishops [53], wearing red and orange (first bishop, from the left to the right), pink and red (second bishop), blue (third bishop) and brown (fourth bishop), long tunics (*sakkos*) and long white stoles (*omophorion*), all decorated with red, pink, yellow, blue and green embroidery and fringes. The background of the painting is blue at the bottom and yellow at the top [50].

2. Materials

The two portions of the wall painting considered in this study are placed in the central apse, one on the left most part (painting A) and one on the right side (painting B). In the painting A, 21 measurement points were taken into account (called "sample" for convenience), specifically, 8 red areas on the side frame that defines the scene and on the clothes of the first and second bishops; 3 light and dark pink areas on their tunics; 2 yellows and 5 blues in the background of the depicted image; and 1 green and 2 whites on the stoles. In painting B, 16 measuring points were considered, namely 5 reds on the side frame and on the shoes of the third bishop; 2 brown areas on the bottom of the tunic of the fourth bishop; 2 greens and 1 white from the stole, 4 blues in the background and 2 greys from the tunic of the third bishop. A map of the measuring points is shown in Figure 1 and a detailed overview of the measuring points and techniques applied for each sample is reported in Table 1.

Figure 1. *Cont.*

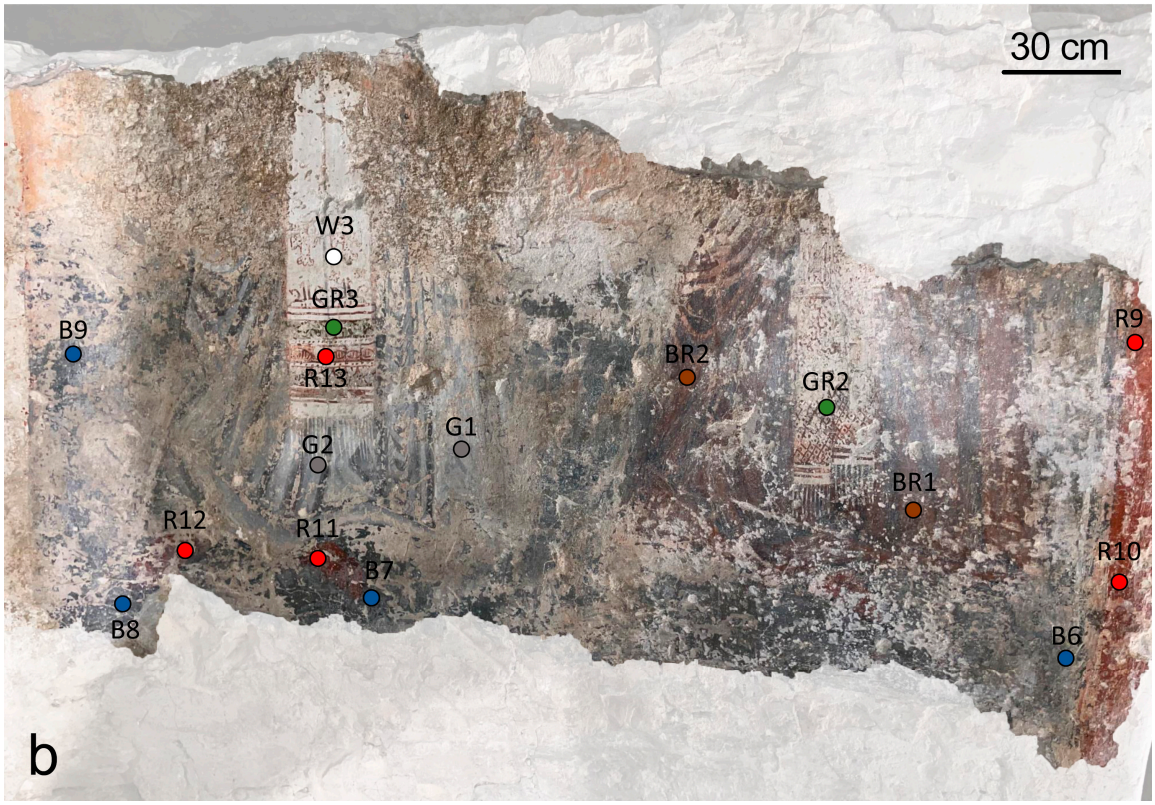

Figure 1. A map of samples in painting A (**a**), and in painting B (**b**).

Table 1. Sample names, grouped by colour, corresponding areas on the paintings and analysis methods (DM: digital microscope) carried out.

	Painting A	Area	Analytical Techniques	Painting B	Area	Analytical Techniques
Red	R1	Left side frame	POM, FORS, XRF	R9	Right side frame	POM, FORS
	R2	1st Bishop, tunic decoration	POM, FORS	R10	Right side frame	POM, FORS, XRF
	R3	1st Bishop, tunic decoration	POM, FORS	R11	3rd Bishop, shoe	POM, FORS, XRF
	R4	1st Bishop, tunic decoration	POM, FORS	R12	3rd Bishop, shoe	POM, FORS
	R5	1st Bishop, tunic decorative band	POM, FORS	R13	3rd Bishop, stole decoration	POM, FORS, XRF
	R6	2nd Bishop, tunic decoration	POM, FORS, XRF			
	R7	2nd Bishop, stole decoration	POM, FORS			
	R8	2nd Bishop, tunic decoration	POM, FORS, XRF			
Brown				BR1	4th Bishop, tunic background	POM, FORS
				BR2	4th Bishop, tunic background	POM, FORS, XRF
Pink	P1	1st Bishop, tunic background	POM, FORS, XRF			
	P2	1st Bishop, tunic rim	POM, FORS			
	P3	2nd Bishop, tunic background	POM, FORS, XRF			

Table 1. *Cont.*

	Painting A	Area	Analytical Techniques	Painting B	Area	Analytical Techniques
Yellow	Y1	Scene background	POM, FORS, XRF			
	Y2	Scene background	POM, FORS			
Green	GR1	1st Bishop, stole decoration	POM, FORS, XRF	GR2	4th Bishop, stole decoration	POM, FORS, XRF
				GR3	4th Bishop, stole decoration	POM, FORS, XRF
Blue	B1	Scene background	POM, FORS	B6	Scene background	POM, FORS
	B2	Scene background	POM, FORS	B7	Scene background	POM, FORS, XRF
	B3	Scene background	POM, FORS, XRF	B8	Scene background	POM, FORS
	B4	Scene background	POM, FORS, XRF	B9	Scene background	POM, FORS, XRF
	B5	Scene background	POM, FORS			
Grey				G1	4th Bishop, tunic decoration	POM, FORS
				G2	4th Bishop, tunic decoration	POM, FORS, XRF
White	W1	1st Bishop, stole background	POM, FORS, XRF	W3	4th Bishop, stole background	POM, FORS, XRF
	W2	2nd Bishop, stole background	POM, FORS			

3. Methods

3.1. Optical Microscopy

For the microscopic observation of pigments included in the surface pictorial layers, the approach used by Fioretti et al. [27] was considered, thanks to which specific markers, such as chromatic, morphological, optical parameters (texture, size, colour, shape, rounding, gloss, edge, general appearance, relationship with the background), were evaluated.

For the microscopic observation of the painting, a Dino-Lite Edge Digital Microscope AM7915MZT was used. This is 10 cm long and is equipped with an automatic magnification ranging between 10 and 220×, a 5-megapixel resolution sensor, a light polariser, 8 switchable LEDs with infrared filter of >650 nm, an extended depth of field and an extended dynamic range system. All the photomicrographs were acquired by DinoCapture 2.0 software (Version 1.5.44) and improved by the white balance tool.

3.2. Reflectance Spectroscopy

The FORS spectral features of painted surfaces were evaluated by means of a custom system by Avantes. It comprised an AvaSpec-ULS2048XL-USB2 model spectrophotometer, an AvaLight-HAL-S tungsten halogen light source and a reflection probe FCR-7UV200-2-ME UV/VIS with a diameter of about 200 µm. The spectral resolution of the instrument was about 1.4 mm and the wavelength range was 200–1100 nm. The recording of spectra was between 300 and 950 nm. For the standardisation of the diffuse reflectance spectra, a WS-2 reflectance standard was adopted. Referring to the experimental condition, the working distance (probe-sample) was about 5 mm and the spot size was 2 mm. For the spectra acquisition, the system was set with 400 ms integration time, with 10 scans for a total acquisition time of 4 s for each spectrum. For the collection of data and their visualisation, processing and comparison with databases, Avasoft 8.0 and Spectragryph [52] software were used, respectively.

3.3. XRF

The composition of painting surfaces was measured, directly on air at room temperature, by a custom portable XRF instrument, made up of a Mini-X with Au target X-ray sources (40 kV and 95 µA) by AMPTEK inc. Bedford, MA, USA, and a silicon drift (SDD)

XR-123 SDD detector (detection area of 25 mm^2, thickness of 500 μm and Be windows (by AMPTEK inc. Bedford, MA, USA) of 12.5 μm. The resolution at 5.9 keV was 135 eV at room temperature. The X-ray beam and detector geometry was fixed at a 90° angle, allowing the reduction of the background on Compton scattering. The working distance, controlled by a laser interferometer, was 15 mm and the outgoing radiation was collimated in a 5 mm beam diameter at the sample surface. The acquisition time for each spectrum was 60 s. For the elaboration of spectra, Spectragryph [54] software was used (version 1.2.15, 2016–2020, developed by Dr. Friedrich Menges, Oberstdorf, Germany). Due to the limits in the element detection when the instrument works in the air, only elements with Z > 14 could be identified. Low counts of the characteristic emission Kα line of Ni, Cu and Zn were always present in the background of the acquired spectra due to the instrument components (slit and case). Considering the operating condition (40 kV and 95 μA), the target (Au) used, the working distance (1.5 cm) and the elements identified—assuming a composition similar to plaster for wall painting, due to the laws of absorption—the depth analysed was less than 300 μm, for, e.g., Fe [55]. The real situation was, of course, much more complicated, and depended on the pigment present and surface coating [56]. Nevertheless, the painting had only one pictorial layer, as had been observed with a microscope in the damaged parts, so the depth of X-ray penetration did not affect the pigment identification.

Looking at the relative intensities of the characteristic emission line for each element, it is necessary to emphasise that there was no relation with the chemical composition but that it resulted from the processes of the interaction-emission photon X-electronic shells of the considered elements.

3.4. Photogrammetric Survey

The 3D digital model of the apse containing the painting was performed by digital photogrammetry, following different experimental expedients, which allowed a reduction of the costs and working time of the survey, and the provision a satisfactory result [47–49]. For the photogrammetric survey of the complete site, including all the masonries of the apses, 925 photographs were collected by means of a Nikon D800 FX (34 MPx, Tokyo, Japan) camera with 800 ISO, equipped with a Nikkor 16 mm FX lens. For the painted surfaces, where a higher resolution of images was mandatory to achieve the aims of this research, a Nikkor 50 mm FX lens was used and 54 frames were captured. In both photogrammetric methods, a LED light (18 W, 5400 K) provided the illumination system. The shooting distance, both for the whole site and for the painted area, was about 1 m and the photo overlapping areas, both vertically and horizontally, were about 60%.

The two obtained digital surveys were easily merged, thanks to the positioning of virtual specific markers.

For the processing of the photo collection, Agisoft Metashape Professional edition software (version 1.4, Agisoft LLC, St. Petersburg, Russia) was utilised to create the 3D model. Starting from the obtained 3D model, the orthophoto (orthorectified photograph) showing the painting was extracted. Thanks to this approach, a high-resolution image of the painting was obtained, ensuring the removal of aberration effects and other optical flaws otherwise generated by a traditional photography or due to of the curved surface of the painting.

For the representation of results on the identified pigments, specific maps were created by means of Adobe Photoshop Professional edition software (version 1.4, Agisoft LLC, St. Petersburg, Russia).

4. Results

4.1. Microscopic Markers

The microscopic observation of samples under the polarised microscope revealed a secondary, more or less encrusted white layer. Referring to the pictorial layers, on the basis of the preliminary macroscopic and microscopic analysis to the naked eye and the definition of the specific microscopic markers [27] reported in Table 2, 10 different types

of pigments or mixtures of pigments were recognised, the latter of which are shown in Figure 2.

The first red (red A) was specific to the orange-red side frame and included a very fine red pigment colouring the matrix, where coarser, round, opaque particles (25 µm) of the same pigment were scattered, then defining a bimodal texture referable to the natural red ochre [27,57–60]. The red B was identified on the lighter area of the tunics of the first and second bishops, while red C was found on the dark red decorations of their tunics and on the shoes of the third bishop. Both reds were composed of a red pigment, marked by bimodal texture due to a finer disperse fraction, and particles (20 µm) of the same pigment. In this case, the morphological features also suggested, the use of red ochre. The difference between red B and red C was due to the presence of black particles, with a tabular shape and a size of 5–15 µm in low amounts in the first case and a higher proportion in the second one. In both cases, the tabular aspect of the pigment suggested the use of vine black [27,61]. In addition, in samples corresponding to the red C, rare particles (20 µm) of a further red, translucent pigment were observed.

Two pink shades were identified on the tunic background of the first and the second bishops. Both pinks were characterised by an extremely fine red pigment, attributable to red ochre, in which rare, tabular black particles were dispersed. In the darker pink (pink A), these particles showed a size lower than 5 µm, whereas in the paler pink (pink B), their size varied between 5 to 20 µm. The black pigment, referable to vine black because of its microscopic features, was certainly more abundant than in pink A, and this would explain its darker colour.

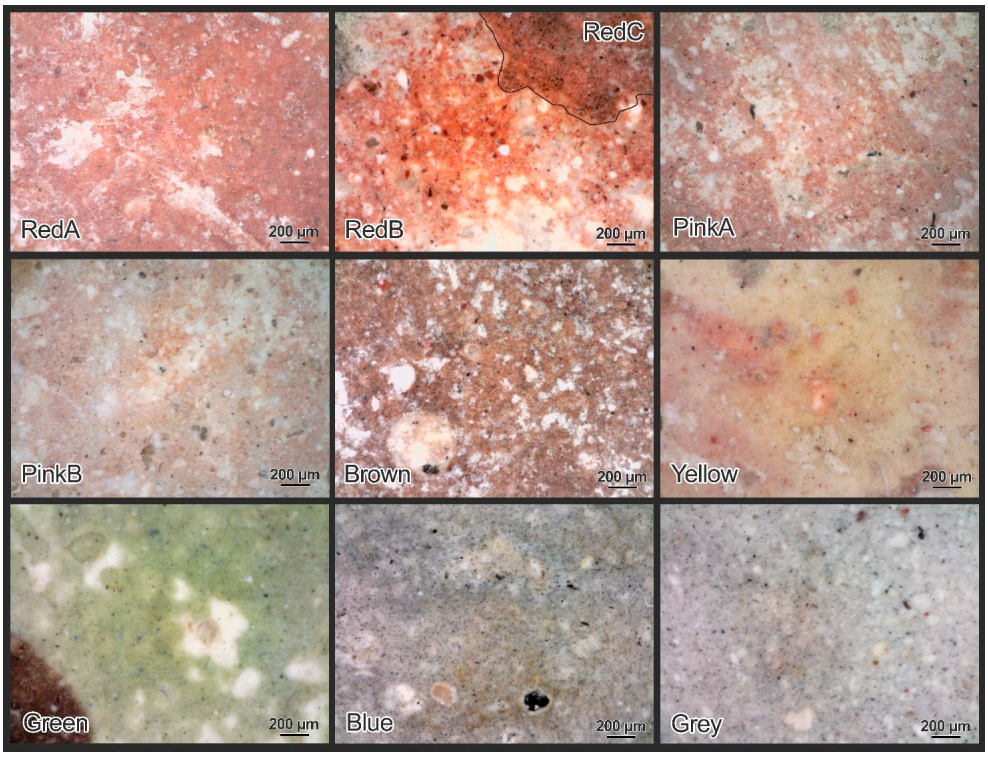

Figure 2. Representative photomicrographs of the 10 different pigments and mixtures observed in the pictorial surfaces, as reported in Table 2.

Table 2. Summary of observations by digital portable microscope, reporting distinctive parameters of each pigment. (*: naked-eye colour; n.v.: not visible; n.i.: not identifiable). For minor components, +: <5%; ++: 5%–20%; +++: >20%.

Colour *	Sample	Attribution	Texture	D Moda (μm)	Colour							Morphology			
					Unpolarised Light			Polarised Light							
					Hue	Saturation	Brightness	Gloss	Hue	Saturation	Brightness	Gloss	Shape	Rounding	Edge	Appearence
Red A	R1, R9, R10	Red ochre	Bimodal	n.v. 25	red red	medium medium-low	medium low	n.v. low	red red	medium medium-low	medium low	n.v. low	n.v. massive	n.v. rounded	n.v. sharp	n.v. intact
Red B	R2, R3, R5, R6, R8	Red ochre	Bimodal	n.v. 20	red red	medium medium-low	medium low	n.v. low	red red	medium medium-low	medium low	n.v. low	n.v. massive	n.v. rounded	n.v. sharp	n.v. intact
		Vine black (+)	Unimodal	5–15	black	medium	medium-high	high	black	low	low	low	tabular	angular	soft	intact
Red C	R4, R7, R11, R12, R13	Red ochre	Bimodal	n.v. 20	red red	medium medium-low	medium low	n.v. low	red red	medium medium-low	medium low	n.v. low	n.v. massive	n.v. rounded	n.v. sharp	n.v. intact
		Vine black (++)	Unimodal	5–15	black	medium	medium-high	high	black	low	low	low	tabular	angular	soft	intact
		n.i. red pigment	Unimodal	20	orange	high	high	high	orange	high	high	high	massive	angular	sharp	intact
Pink A	P3	Hematite or red ochre (?)	Unimodal	n.v.	red	medium	medium	n.v.	red	medium	medium	n.v.	n.v.	n.v.	n.v.	n.v.
		Vine black (+)	Unimodal	<5	black	medium	medium-high	high	black	low	low	low	tabular	angular	soft	intact
Pink B	P1, P2	Hematite or red ochre (?)	Unimodal	n.v.	red	medium	medium	n.v.	red	medium	medium	n.v.	n.v.	n.v.	n.v.	n.v.
		Vine black (++)	Unimodal	5–20	black	medium	medium-high	high	black	low	low	low	tabular	angular	soft	intact
Brown	BR1, BR2	Red ochre	Bimodal	n.v. 15	red red	medium medium-low	medium low	n.v. low	red red	medium medium-low	medium low	n.v. low	n.v. massive	n.v. rounded	n.v. sharp	n.v. intact
		Vine black (+)	Unimodal	<10	black	medium	medium-high	high	black	low	low	low	tabular	angular	soft	intact
Yellow	Y1, Y2	Yellow ochre	Bimodal	n.v. <10	yellow yellow	low low	low low	n.v. low	yellow yellow	low low	low low	n.v. low	n.v. massive	n.v. rounded	n.v. sharp	n.v. intact
		Red ochre	Bimodal	n.v. <10	red red	medium medium-low	medium low	n.v. low	red red	medium medium-low	medium low	n.v. low	n.v. massive	n.v. rounded	n.v. sharp	n.v. intact
Green	GR1, GR2, GR3	Green earth	Bimodal	n.v. <10	green green	low low	medium low	n.v. low	green green	low low	low low	n.v. low	n.v. massive	n.v. rounded	n.v. sharp	n.v. intact
		n.i. blue pigment	Unimodal	<10	blue	high	high	high	blue	high	high	low	massive	mixed	sharp	intact
Blue	B1, B2, B3, B4, B5, B6, B7, B8, B9	Vine black (+++)	Unimodal	<10	black	medium	medium-high	high	black	low	low	low	tabular	angular	soft	intact
		n.i. yellow pigment	Unimodal	<10	yellow	n.v.	n.v.	n.v.	n.v.	n.v.	n.v.	n.v.	n.v.	n.v.	n.v.	n.v.
Grey	G1, G2	Vine black (++)	Unimodal	<10	black	medium	medium-high	high	black	low	low	low	tabular	angular	soft	intact
		Yellow ochre (coarser fraction)	Unimodal	20	yellow	low	low	low	yellow	low	low	low	massive	rounded	sharp	intact

On the tunic of the fourth bishop, the brown painting was composed of a very dark red pigment, with a bimodal texture, due to a finer fraction in the matrix and opaque, rounded particles (15 μm), which would appear to be red ochre. A black pigment characterised by a tabular shape and a size between a few to 10 μm, referable to the vine black, was added.

The yellow areas of the background of painting A were characterised by an irregular yellow and pink matrix, where yellow, opaque and rounded particles (<10 μm) and red, opaque and rounded particles (<10 μm) were dispersed. Such features suggest the use of a mix composed of yellow [27,57–59] and red ochre.

The microscopic observation of the green stole decorations highlighted a very fine green pigment where scattered opaque and rounded particles (<10 μm) of the same colour were well visible, referable to green earth [27]. Likewise, there were several recognisable fine particles (<10 μm) of a blue pigment, whose identification in this specific case cannot be made on the basis of the microscopic features.

The blue colour of the background of painting A was due to a black pigment showing fine particles (<10 μm), marked by tabular shape, and a very fine yellow pigment. Conversely, for the first pigment, the microscopic features suggested the use of vine black; for the yellow, an identification hypothesis cannot be given.

Additionally, regarding the grey paintings on the tunic of the third bishop, black, fine (<10 μm) and tabular particles mixed with a small amount of yellow, rounded and opaque particles (20 μm) were observed. They are likely to be vine black and yellow ochre, respectively.

For the white areas on the stoles, the microscopic analysis was not very indicative, as it did not enable the recognition of the pigment particles.

4.2. Reflectance Features

All the points observed by the microscope were analysed by FORS, and the results of which are summarised in Table 3. Results of FORS analysis indicated, for red A and red B (Figure 3a), two similar reflectance spectra characterised by an s-shape, a reflectance maximum centred at ~745 nm and an inflection point at ~580 nm, all ascribable to the red ochre [19,20,22,23,27]. Red C had a curve (Figure 3a) showing spectral features comparable to the previous case and to red ochre; however, it was marked by a shift of about 25 nm, both in the reflectance maximum (~720 nm) and in the inflection point (~565 nm). They are likely attributable to red ochre, as the shift was possibly connected to the mixing with black particles created by the artist for this pictorial layer [27].

Reflectance spectra of pink A and pink B (Figure 3b) were characterised by an s-shape and by a reflectance band at ~750 nm, indicating the use of red ochre [19,27,60].

For the brown pictorial layer, the curve (Figure 3c) displayed an irregular trend due to a swift increase in reflectance in the wavelength region between 500 and 600 nm, an inflection point centred at ~565 nm and a flattening after 600 nm, possibly attributable to the strong contribution of the black pigment in the mixture.

Table 3. FORS spectral features of samples (*: naked-eye colour).

Colour *	Sample	FORS Spectral Features	Attribution
Red A	R1, R9, R10	~745 nm (max); ~580 nm (i.p.)	Red ochre
Red B	R2, R3, R5, R6, R8	~745 nm (max); ~580 nm (i.p.)	Red ochre
Red C	R4, R7, R11, R12, R13	~720 nm (max); ~565 nm	Red ochre
Pink A	P3	~750 nm (max)	Red ochre
Pink B	P1, P2	~750 nm (max)	Red ochre
Brown	BR1, BR2	~565 nm (i.p.)	Red ochre
Yellow	Y1, Y2	~770 nm (max)	Yellow ochre
Green	GR1, GR2, GR3	~570 nm (max); ~750 nm (min); absorbance band 600–680 nm	Green earth + Egyptian blue

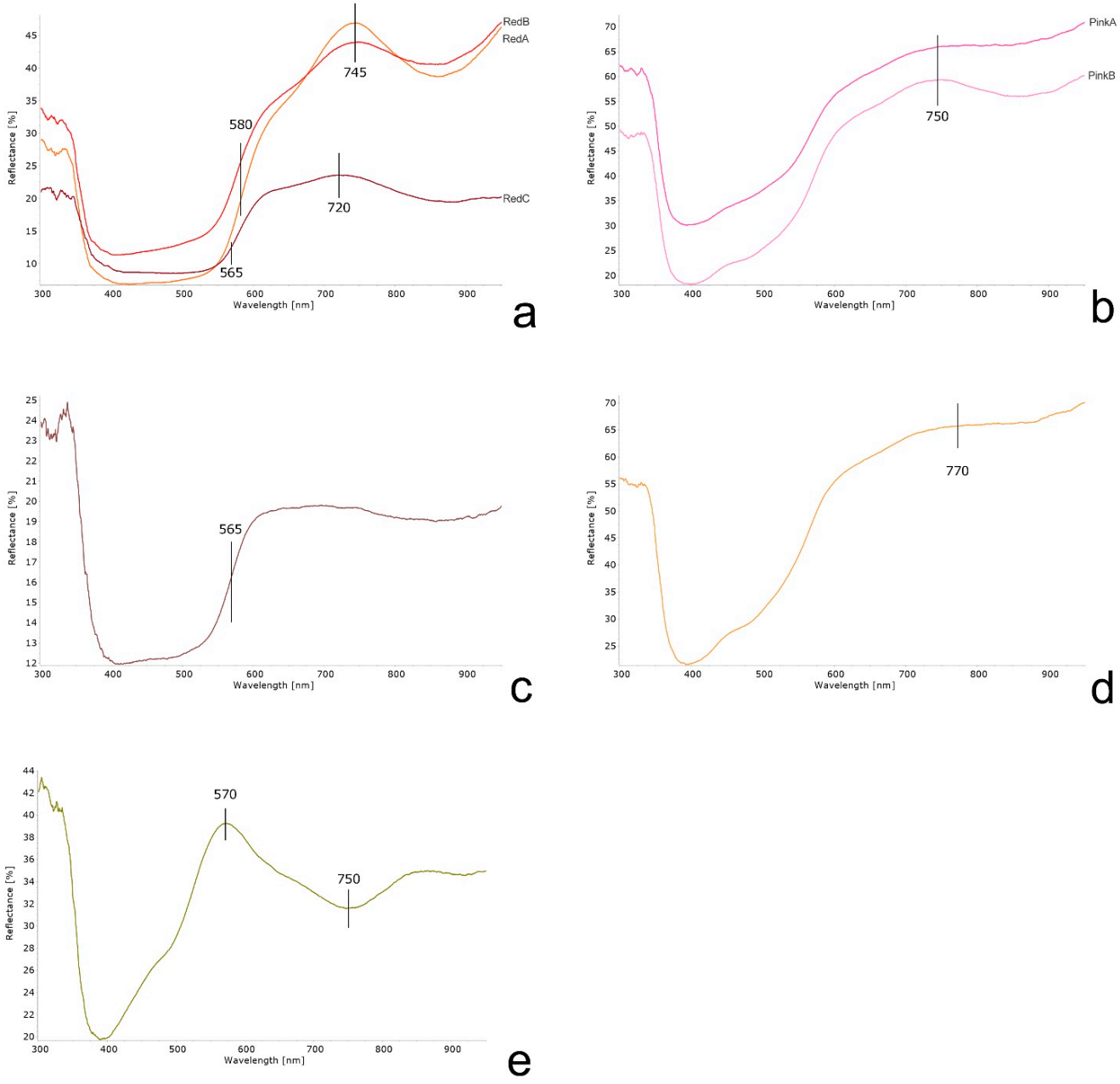

Figure 3. Representative FORS reflectance spectra for three reds (**a**), two pinks (**b**), brown (**c**), yellow (**d**) and green (**e**) areas of the painting.

The reflectance curves of the yellow areas (Figure 3d) were marked by an s-shape and a maximum at ~770 nm, fitting the typical spectrum of yellow ochre [19,20,22,23,27].

The green colour curve (Figure 3e) showed the reflectance spectrum of green earth [27,62] characterised by a maximum at ~570 nm, even if two weak absorbance bands, the first between 600 and 680 nm and the second at ~750 nm, indicate the presence of Egyptian blue [63]. As expected, for grey, dark blue and white areas, the reflectance spectra did not point out specific spectral features and therefore, they were not useful for the pigment identification.

4.3. Elemental Composition

The XRF analyses were performed on 20 representative points, whose results are summarised in Table 4.

Table 4. Elemental composition, obtained by XRF (+: major elements; -: minor elements; tr: traces), of samples (*: naked-eye colour).

Colour *	Sample	XRF Chemical Composition	Attribution
Red A	R1	Ca (+), Fe (-), S (-), Si (tr), K (tr), Ti (tr)	Red ochre
Red B	R6, R8	Ca (+), Fe (-), S (-), Si (tr), K (tr), Ti (tr)	Red ochre
Red C	R4, R11, R13	Ca (+), Fe (-), S (-), Si (tr), K (tr), Ti (tr)	Red ochre
Pink A	P3	Ca (+), Fe (-), K (tr), Si (tr), Ti (tr)	Red ochre
Pink B	P1	Ca (+), Fe (-), K (tr), Si (tr)	Red ochre
Brown	BR2	Ca (+), Fe (-), Si (tr), K (tr), Ti (tr)	Red ochre
Yellow	Y1	Ca (+), Fe (-), K (tr)	Yellow ochre
Green	GR1, GR2, GR3	Ca (+), Fe (-), S (tr), Si (tr), Cu (tr)	Green earth + Egyptian blue
Blue	B3, B4, B7, B9	Ca (+), Fe (tr), K (tr)	Yellow ochre
Grey	G2	Ca (+), Fe (tr), K (tr)	Yellow ochre
White	W1, W3	Ca (+)	–

The presence in all the spectra of low traces of Au, Ni, Cu, Zn and Ar was connected to the instrument setup and traces of S were imputable to the presence of sulphates as degradation products already visible to the naked eye.

For red areas (red A, red B and red C), XRF spectra (Figure 4a) were highly comparable and showed peaks of Ca, Fe, Si and K, suggesting the occurrence of red ochre as the single pigment. A similar composition was found in both pink (pink A and pink B) and in yellow areas, where the predominant contribution of Fe should indicate the use of red ochre and yellow ochre, respectively.

Additionally, in the brown area, the presence of Ca, Fe, K and Ti are likely ascribable to the use of red ochre. In all these cases, traces of Ti, K and Mn are likely related to red ochre, which generally, together with the chromophore iron oxides, contains additional phases, such as anatase (TiO_2) [64].

For green areas, XRF spectra (Figure 4b) showed peaks of Ca and Fe and traces of S, Si and a slightly higher peak of Cu than the other samples. The elemental composition likely indicates the use of green earth, and the Cu-based pigment could correspond to the Egyptian blue [63], as also highlighted in FORS spectrum. The very low intensity of the Cu peak is justified by the very limited quantity of blue pigment, already observed by the microscope.

Conversely, in the blue areas of the scene background, the composition of the pictorial layer (Figure 4c) was essentially due to Ca, Fe, Mn and K, suggesting the addition of a Fe-based pigment, possibly yellow ochre, as revealed in the microscopic observation. Even if the spectrum showed a copper peak, its low intensity and, especially, the clear absence of blue pigment particles under the microscope, would suggest that it was related to the instrument setup and not to the presence of a blue pigment.

A highly comparable spectrum was produced for the grey area, also in this case, revealing the use of a very limited amount of ochre in the black pigment. For the white paintings, XRF spectra revealed the presence of Ca as the main element, which could be ascribable to the plaster or to a Ca-based white pigment.

4.4. Visual Representation of Results

By means of the digital photogrammetric technique, the 3D model of the church (Figure 5) ruins was obtained, and two orthophotos of the two painted fragments (painting A and painting B) were extrapolated.

The digital product is undoubtedly an important milestone that has made it possible to overcome, among other things, the lack of useful space for taking photographs of curved painting surfaces. The result of the mapping, by overlapping graphic layers on the orthophotos, allowed the results to be represented graphically (Figure 6).

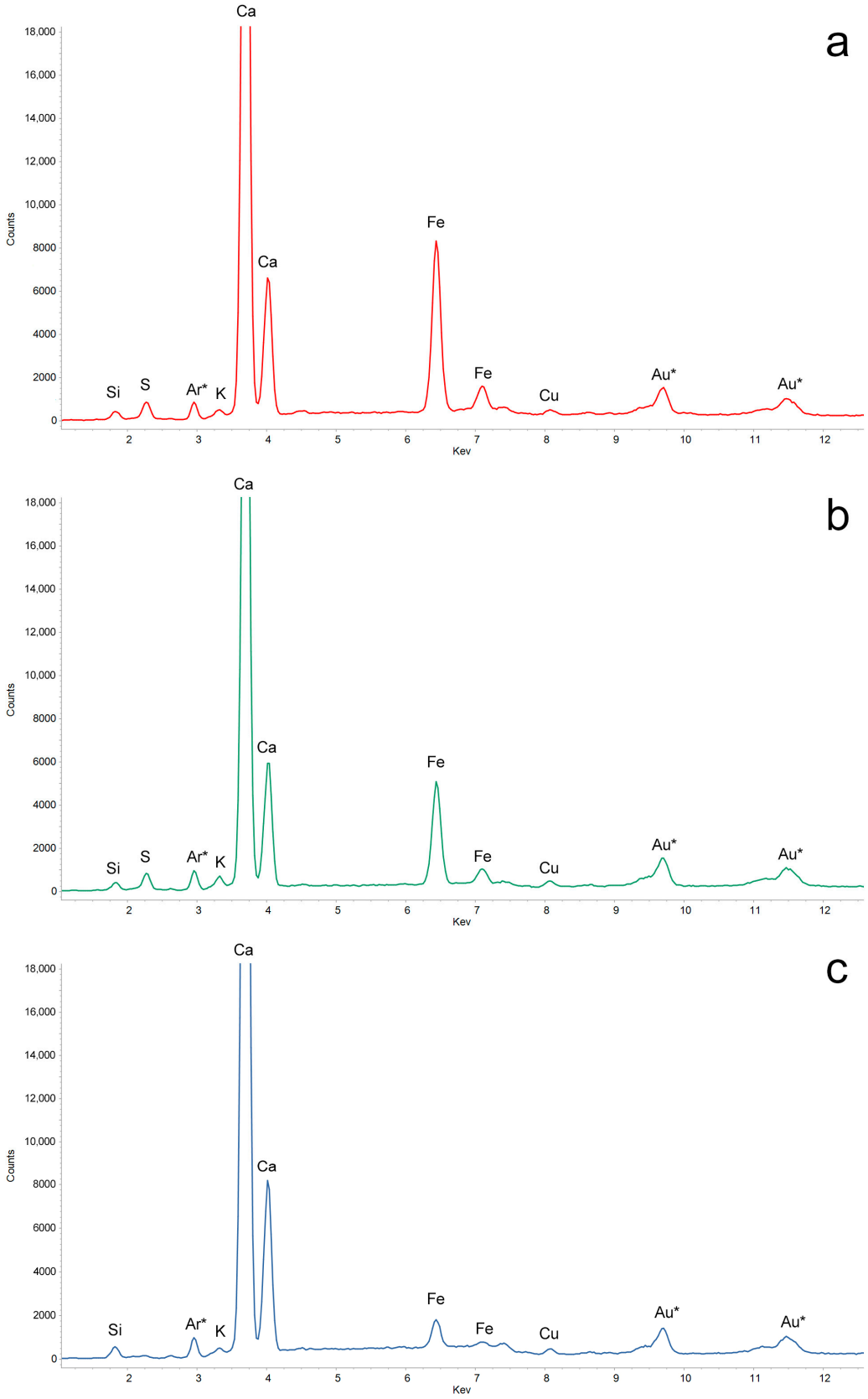

Figure 4. Representative XRF spectra for red (**a**), green (**b**) and blue paintings (**c**). * indicates elements connected to the instrument setup.

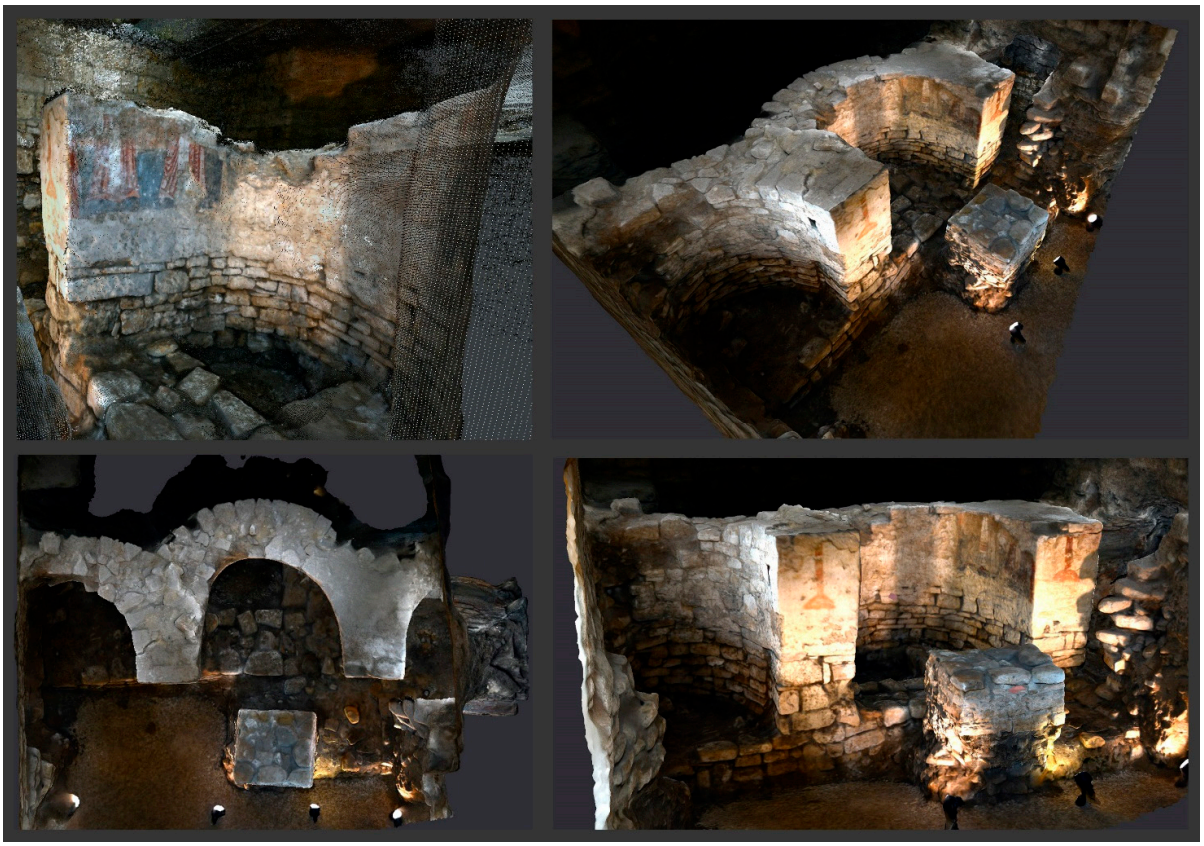

Figure 5. Photogrammetric survey of the archaeological site apses.

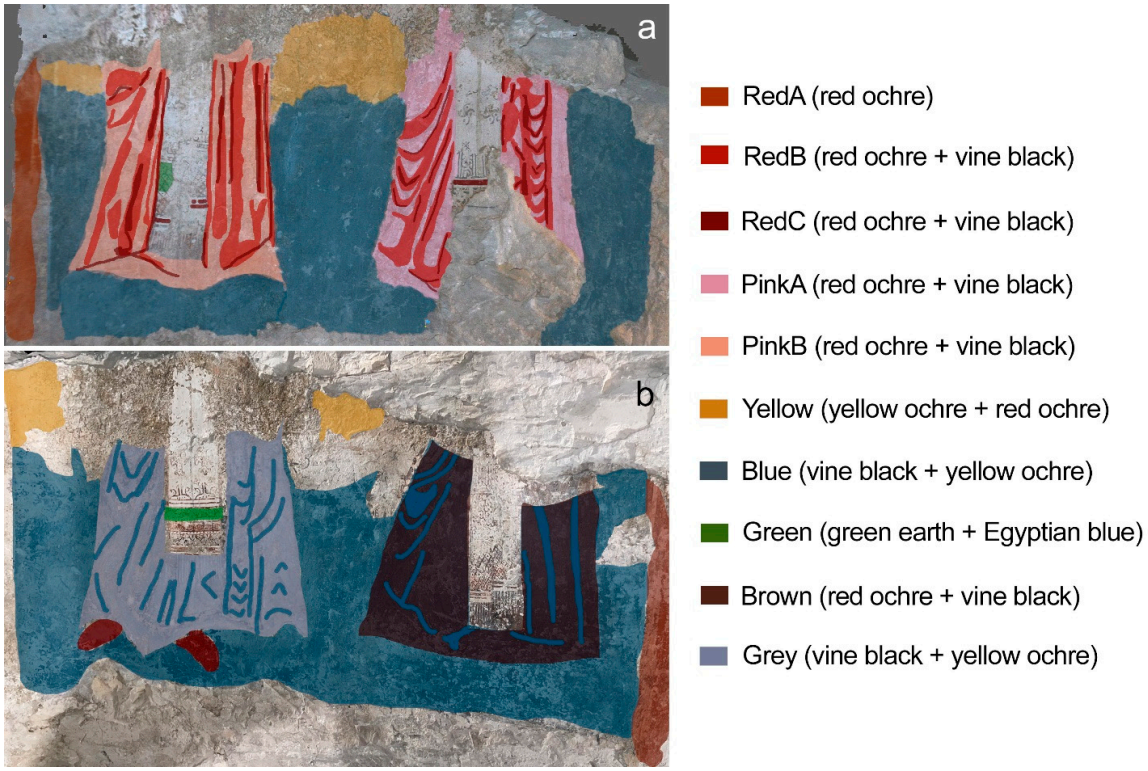

Figure 6. Mapping of pigments and mixtures identified in the painting A (**a**) and B (**b**), obtained overlapping specific layers on the photogrammetric orthophotos.

5. Discussion

The comparison of the obtained results enabled the identification of the pigments used in the fragments of the apse wall painting in the Byzantine church under Palazzo Simi. They are mostly common and inexpensive pigments, extremely widespread in the medieval mural paintings of the region [1,4,8], but more generally, in the Byzantine wall pictorial tradition [65–67].

Specifically, 11 different "recipes" were recognised, some consisting of a single pigment, others of two pigments mixed in different proportions in order to obtain different chromatic effects. The three red colours (red A, red B and red C), brown and the two pinks, used for the bishops' tunics and for the side frames of the painting, were substantially composed of red ochre as the main pigment. It was easily recognised by optical microscopy due to its textural parameters, by FORS for the s-shape and for the absorbance peak at ~745 nm and by XRF for its typical chemical composition. Furthermore, although the unimodal texture of the red pigment found by microscopy in the pink layers (pink A and pink B) suggested the presence of hematite [27], the latter was definitively excluded due to the presence of typical ochre impurities revealed by XRF analysis.

The same composition was found by XRF on the yellow areas of the painting scene background, where the presence of yellow ochre was distinguished thanks to the absorbance peak centred at ~770 nm in the FORS spectrum and, clearly, thanks to optical microscopy.

In red, yellow, brown and pink areas, the presence of the black pigment was intentional, in order to darken the predominant colour; moreover, its absence in some areas (green, white and red A) should exclude the environmental origin (smoke from candles, dust, anthropic pollution) of the black particles.

The microscopic analysis of the green areas in the decorations of the stoles immediately brought to light the presence of a green pigment, referable to green earth, mixed with rare fine particles of a blue pigment. It was recognised as Egyptian blue, thanks to the FORS curve [63] and the presence of a slightly higher amount of copper than in the other samples. In this case, the contribution of microscopy was fundamental, making it possible to avoid erroneously attributing the presence of copper to a green pigment such as malachite [68]. The mixture consisting of green and blue Egyptian earth is not very common in the medieval paintings of the region, even though it was found in the Festoni Tomb in Taranto (Italy) [1].

In the blue and grey areas of the background and of the third bishop's tunic, respectively, the FORS results did not provide useful indications to recognise the pigments, as curves appeared flat and diagnostic spectral features were missing. Conversely, thanks to the comparison of microscopic observation and XRF spectra, a black pigment showing blue shades (possibly vine black) and yellow ochre were identified. Furthermore, the higher amount of the black pigment in the blue areas than in the grey areas would explain the darker colour. The mixing of black and yellow pigments in different ratios was found elsewhere in the region, for example, in the St. Maria Veterana church in Triggiano (Bari, Italy) [4] and in the Santi Stefani crypt at Vaste (Lecce, Italy) [5], proving this *modus operandi* in the medieval local painting tradition. The XRF spectra of the white areas, corresponding to the bishops' stoles, showed the sole presence of calcium, thus suggesting the hypothesis of a white pigment based on calcium carbonate or hydroxide [69] or the absence of a real pictorial layer, and that the decorations of the stoles were applied directly on the plaster.

The considered approach enabled the attainment of significant information on the chromatic palette used by the artists and contribution to understanding of the raw materials and of the *modus operandi* of the medieval wall painting tradition of the Puglia region. The portable microscope proved to be both very effective for a preliminary observation of the pictorial layers, and an excellent starting point for choosing and carrying out further investigation methods. Although FORS could be considered effective in the characterisation of pigments, among its weaknesses, it is worth mentioning the difficulty in evaluating more complex mixes of pigments and the poor efficacy for black and white pigments, which tend to have a flat spectrum. Similarly, portable XRF does not enable the evaluation the lightest elements, making it impossible to identify the pigments. However, the comparison of the

results obtained from these three non-invasive methods proved suitable for identifying the raw materials used for the pictorial layers with good reliability.

Furthermore, this approach enabled the provision of information on the compositions of the most superficial layers of the wall paintings, although it is not useful for the characterisation of multi-layered paintings. In fact, for the stratigraphic analysis, destructive sampling and a more in-depth observation of the cross-sections under the reflected-light microscope are necessary. In this way, it is also possible to carry out detailed analyses on each pigment particle by using analytical techniques equipped with a microscope such as, for example, μRaman and SEM-EDS.

6. Conclusions

The non-invasive approach applied, based on the combined use of optical microscopy, FORS and XRF, made it possible to identify, for the first time, the pictorial materials used in the wall painting of the Byzantine church under Palazzo Simi.

Experimental data highlighted the presence of common pigments in the wall painting, especially from the Middle Ages of the Puglia region, including red and yellow ochres, green earth and vine black. Furthermore, some mixes of pigments confirmed the custom of artists, working locally at that time, to blend two or more common pigments to obtain specific chromatic tones.

The presented study first of all confirmed the importance of a preliminary observation through a portable microscope equipped with a polariser, which enabled the acquisition of general information on the pictorial surfaces, in terms of the morphology, shape, size and colour of the pigment particles.

Notably, the complementary quality of the three analytical techniques underlying the characterisation of the paintings, as in all cases, helped to resolve doubts and, very likely, to define the composition of the pictorial layers.

Finally, thanks to photogrammetry, a digital survey of the site was carried out both for dissemination and study purposes. In fact, the results obtained from the study on pigments were graphically represented on specific orthophotos extracted from the 3D model, thus facilitating the comprehension for non-experts and enriching the knowledge of this very valuable archaeological site in the city of Bari.

Author Contributions: Conceptualisation, G.F.; software: G.F. and S.C.; methodology, G.F., S.C. and G.T.; formal analysis: G.F., S.C. and G.T.; investigation, G.F. and G.T.; writing—original draft; preparation, G.F.; writing—review and editing, G.F., G.T. and G.E.; visualisation, G.F. and G.T.; supervision, G.F. and G.E.; funding acquisition: G.E. All authors have read and agreed to the published version of the manuscript.

Funding: The research was financially supported by the Italian Ministry of University and Research (Italy), through the National Operational Program (PON) for Research and Innovation 2014–2020 (Project AIM1815472-Activity 2-Line 1).

Institutional Review Board Statement: Not applicable.

Informed Consent Statement: Not applicable.

Data Availability Statement: Data are contained within the article.

Acknowledgments: The authors would like to thank the Authority for Archaeology, Fine Arts and Landscape for the metropolitan city of Bari—Italian Ministry of Culture for the permission to carry out the non-invasive analysis and to reproduce the research results.

Conflicts of Interest: The authors declare no conflict of interest.

References

1. Calia, A.; Giannotta, M.T. *La Tomba dei Festoni di via Crispi a Taranto: Individuazione e Riconoscimento dei Pigmenti Utilizzati Nelle Pitture*; D'Amico, C., Ed.; Pàtron Editore: Bologna, Italy, 2005; pp. 271–278.
2. Calia, A.; Melica, D.; Quarta, G. I Dipinti Murali Del Tempietto: Materiali Costituenti e Tecniche Esecutive. In *Masseria Seppannibale Grande in Agro di Fasano (BR)*; Bertelli, G., Lepore, G., Eds.; Adda Editore: Bari, Italy, 2011; pp. 195–206.

3. Capitanio, D.; Laviano, R.; Menga, A.; Meo-Evoli, N.; Vona, F.; Vurro, F. Intonaci e Pitture Murali Dell'ipogeo Di S. Matteo All'Arena, Monopoli (Bari). In *Sulle Pitture Murali*; Arcadia Ricerche: Marghera-Venezia, Italy, 2005; pp. 1137–1146.
4. Fioretti, G.; Raneri, S.; Pinto, D.; Mignozzi, M.; Mauro, D. The Archaeological Site of St. Maria Veterana (Triggiano, Southern Italy): Archaeometric Study of the Wall Paintings for the Historical Reconstruction. *J. Archaeol. Sci. Rep.* **2020**, *29*, 102080. [CrossRef]
5. Fico, D.; Pennetta, A.; Rella, G.; Savino, A.; Terlizzi, V.; De Benedetto, G.E. A Combined Analytical Approach Applied to Medieval Wall Paintings from Puglia (Italy): The Study of Painting Techniques and Its Conservation State: Study of Painting Techniques and Its Conservation State. *J. Raman Spectrosc.* **2016**, *47*, 321–328. [CrossRef]
6. Calia, A.; Giorgi, M.; Quarta, G.; Masieri, M. *Le Pitture Della Cripta Del Gonfalone a Tricase (Lecce): Problematiche Storico-Artistiche e Contributo Alla Identificazione Dei Pigmenti Attraverso FRX Portatile*; Fioretti, G., Ed.; Edizioni Fondazione Pasquale Battista: Bari, Italy, 2021; pp. 125–132.
7. De Benedetto, G.E.; Fico, D.; Margapoti, E.; Pennetta, A.; Cassiano, A.; Minerva, B. The Study of the Mural Painting in the 12th Century Monastery of Santa Maria Delle Cerrate (Puglia-Italy): Characterization of Materials and Techniques Used: Study of Painting at the Santa Maria Delle Cerrate Church. *J. Raman Spectrosc.* **2013**, *44*, 899–904. [CrossRef]
8. Fioretti, G.; Garavelli, A.; Germinario, G.; Pinto, D. Archaeometric Study of Wall Rock Paintings from the Sant'Angelo in Criptis Cave, Santeramo in Colle, Bari: Insights on the Rupestrian Decorative Art in Apulia (Southern Italy). *Archaeol. Anthr. Sci.* **2021**, *13*, 168. [CrossRef]
9. Vasco, G.; Serra, A.; Manno, D.; Buccolieri, G.; Calcagnile, L.; Buccolieri, A. Investigations of Byzantine Wall Paintings in the Abbey of Santa Maria Di Cerrate (Italy) in View of Their Restoration. *Spectrochim. Acta Part A Mol. Biomol. Spectrosc.* **2020**, *239*, 118557. [CrossRef]
10. Piovesan, R.; Mazzoli, C.; Maritan, L.; Cornale, P. Fresco and lime-paint: An experimental study and objective criteria for distinguishing between these painting techniques. *Archaeometry* **2012**, *54*, 723–736. [CrossRef]
11. Jia, Y.; Zhang, L.; Xu, Y.; Ye, L.; Gu, L.; Chang, L.; Wang, W.; Dai, Y.; Bai, J. Multi-Analytical Investigations on a Tomb Mural Painting of the Yuan Dynasty in Chongqing, China. *Vib. Spectrosc.* **2023**, *124*, 103475. [CrossRef]
12. Duran, A.; Perez-Rodriguez, J.L.; Jimenez de Haro, M.C.; Franquelo, M.L.; Robador, M.D. Analytical Study of Roman and Arabic Wall Paintings in the Patio De Banderas of Reales Alcazares' Palace Using Non-Destructive XRD/XRF and Complementary Techniques. *J. Archaeol. Sci.* **2011**, *38*, 2366–2377. [CrossRef]
13. Garofano, I.; Perez-Rodriguez, J.L.; Robador, M.D.; Duran, A. An Innovative Combination of Non-Invasive UV–Visible-FORS, XRD and XRF Techniques to Study Roman Wall Paintings from Seville, Spain. *J. Cult. Herit.* **2016**, *22*, 1028–1039. [CrossRef]
14. Dal Fovo, A.; Mazzinghi, A.; Omarini, S.; Pampaloni, E.; Ruberto, C.; Striova, J.; Fontana, R. Non-Invasive Mapping Methods for Pigments Analysis of Roman Mural Paintings. *J. Cult. Herit.* **2020**, *43*, 311–318. [CrossRef]
15. Blümich, B.; Del Federico, E.; Jaschtschuk, D.; Küppers, M.; Fallon, K.; Steinfeld, A.; Tomassini, P. Nondestructive Analysis of Wall Paintings at Ostia Antica. *Heritage* **2021**, *4*, 4421–4438. [CrossRef]
16. de Queiroz Baddini, A.L.; de Paula Santos, J.L.V.; Tavares, R.R.; de Paula, L.S.; da Costa Araújo Filho, H.; Freitas, R.P. PLS-DA and Data Fusion of Visible Reflectance, XRF and FTIR Spectroscopy in the Classification of Mixed Historical Pigments. *Spectrochim. Acta Part A Mol. Biomol. Spectrosc.* **2022**, *265*, 120384. [CrossRef] [PubMed]
17. Larsen, R.; Coluzzi, N.; Cosentino, A. Free Xrf Spectroscopy Database of Pigments Checker. *Int. J. Conserv. Sci.* **2016**, *7*, 659–668.
18. Cheilakou, E.; Troullinos, M.; Koui, M. Identification of Pigments on Byzantine Wall Paintings from Crete (14th Century AD) Using Non-Invasive Fiber Optics Diffuse Reflectance Spectroscopy (FORS). *J. Archaeol. Sci.* **2014**, *41*, 541–555. [CrossRef]
19. Cosentino, A. FORS Spectral Database of Historical Pigments in Different Binders. *e-Cons* **2014**, *2*, 57–68. [CrossRef]
20. Cavaleri, T.; Giovagnoli, A.; Nervo, M. Pigments and Mixtures Identification by Visible Reflectance Spectroscopy. *Procedia Chem.* **2013**, *8*, 45–54. [CrossRef]
21. Delaney, J.K.; Ricciardi, P.; Glinsman, L.D.; Facini, M.; Thoury, M.; Palmer, M.; de la Rie, E.R. Use of Imaging Spectroscopy, Fiber Optic Reflectance Spectroscopy, and X-Ray Fluorescence to Map and Identify Pigments in Illuminated Manuscripts. *Stud. Conserv.* **2014**, *59*, 91–101. [CrossRef]
22. Corradini, M.; de Ferri, L.; Pojana, G. Fiber Optic Reflection Spectroscopy–Near-Infrared Characterization Study of Dry Pigments for Pictorial Retouching. *Appl. Spectrosc.* **2021**, *75*, 445–461. [CrossRef] [PubMed]
23. Picollo, M.; Bacci, M.; Casini, A.; Lotti, F.; Porcinai, S.; Radicati, B.; Stefani, L. Fiber Optics Reflectance Spectroscopy: A Non-Destructive Technique for the Analysis of Works of Art. In *Optical Sensors and Microsystems*; Martellucci, S., Chester, A.N., Mignani, A.G., Eds.; Kluwer Academic Publishers: Boston, MA, USA, 2002; pp. 259–265. [CrossRef]
24. Villafana, T.; Edwards, G. Creation and Reference Characterization of Edo Period Japanese Woodblock Printing Ink Colorant Samples Using Multimodal Imaging and Reflectance Spectroscopy. *Herit. Sci.* **2019**, *7*, 94. [CrossRef]
25. Galli, A.; Caccia, M.; Bonizzoni, L.; Gargano, M.; Ludwig, N.; Poldi, G.; Martini, M. Deep inside the Color: How Optical Microscopy Contributes to the Elemental Characterization of a Painting. *Microchem. J.* **2020**, *155*, 104730. [CrossRef]
26. Lee, N.R.; Kim, S.J.; Moon, D.H. Non-Invasive Mineral Analysis of Pigments of Wall Paintings in the Sungseonjeon Hall. *Geosci. J.* **2022**, *27*, 161–176. [CrossRef]
27. Fioretti, G.; Clausi, M.; Eramo, G.; Longo, E.; Monno, A.; Pinto, D.; Tempesta, G. A Non-Invasive and Sustainable Characterization of Pigments in Wall Paintings: A Library of Apulian Colors. *Heritage* **2023**, *6*, 1567–1593. [CrossRef]
28. Aicardi, I.; Chiabrando, F.; Maria Lingua, A.; Noardo, F. Recent Trends in Cultural Heritage 3D Survey: The Photogrammetric Computer Vision Approach. *J. Cult. Herit.* **2018**, *32*, 257–266. [CrossRef]

29. McCarthy, J. Multi-Image Photogrammetry as a Practical Tool for Cultural Heritage Survey and Community Engagement. *J. Archaeol. Sci.* **2014**, *43*, 175–185. [CrossRef]
30. Noardo, F. Architectural Heritage Semantic 3D Documentation in Multi-Scale Standard Maps. *J. Cult. Herit.* **2018**, *32*, 156–165. [CrossRef]
31. Drap, P.; Merad, D.; Boi, J.-M.; Seinturier, J.; Peloso, D.; Reidinger, C.; Vannini, G.; Nucciotti, M.; Pruno, E. Photogrammetry for Medieval Archaeology: A Way to Represent and Analyse Stratigraphy. In Proceedings of the 2012 18th International Conference on Virtual Systems and Multimedia, Milan, Italy, 2–5 September 2012; IEEE: Milan, Italy, 2012; pp. 157–164. [CrossRef]
32. Pierdicca, R. Mapping Chimu's Settlements for Conservation Purposes Using UAV and Close Range Photogrammetry. The Virtual Reconstruction of Palacio Tschudi, Chan Chan, Peru. *Digit. Appl. Archaeol. Cult. Herit.* **2018**, *8*, 27–34. [CrossRef]
33. José Luis, P.-G.; Antonio Tomás, M.-C.; Vicente, B.-C.; Alejandro, J.-S. Photogrammetric Studies of Inaccessible Sites in Archaeology: Case Study of Burial Chambers in Qubbet El-Hawa (Aswan, Egypt). *J. Archaeol. Sci.* **2019**, *102*, 1–10. [CrossRef]
34. Cantini, L.; Previtali, M.; Moioli, R.; Della Torre, S. The Mensiochronology Analysis Supported by New Advanced Survey Techniques: Field Tests in Milanese Area. *Int. Arch. Photogramm. Remote Sens. Spat. Inf. Sci.* **2019**, *XLII-2/W11*, 359–365. [CrossRef]
35. Aragón, E.; Munar, S.; Rodríguez, J.; Yamafune, K. Underwater Photogrammetric Monitoring Techniques for Mid-Depth Shipwrecks. *J. Cult. Herit.* **2018**, *34*, 255–260. [CrossRef]
36. Doležal, M.; Vlachos, M.; Secci, M.; Demesticha, S.; Skarlatos, D.; Liarokapis, F. Understanding Underwater Photogrammetry for Maritime Archaeology through Immersive Virtual Reality. *Int. Arch. Photogramm. Remote Sens. Spat. Inf. Sci.* **2019**, *XLII-2/W10*, 85–91. [CrossRef]
37. Siebke, I.; Campana, L.; Ramstein, M.; Furtwängler, A.; Hafner, A.; Lösch, S. The Application of Different 3D-Scan-Systems and Photogrammetry at an Excavation—A Neolithic Dolmen from Switzerland. *Digit. Appl. Archaeol. Cult. Herit.* **2018**, *10*, e00078. [CrossRef]
38. Berquist, S.; Spence-Morrow, G.; Gonzalez-Macqueen, F.; Rizzuto, B.; Álvarez, W.Y.; Bautista, S.; Jennings, J. A New Aerial Photogrammetric Survey Method for Recording Inaccessible Rock Art. *Digit. Appl. Archaeol. Cult. Herit.* **2018**, *8*, 46–56. [CrossRef]
39. Sapirstein, P. A High-Precision Photogrammetric Recording System for Small Artifacts. *J. Cult. Herit.* **2018**, *31*, 33–45. [CrossRef]
40. Andreu, J.; Serrano, P. Contributions of the Digital Photogrammetry and 3D Modelling of Roman Inscriptions to the Reading of Damaged Tituli: An Example from the Hispania Tarraconensis (Castiliscar, Saragossa). *Digit. Appl. Archaeol. Cult. Herit.* **2019**, *12*, e00091. [CrossRef]
41. Salagean-Mohora, I.; Anghel, A.A.; Frigura-Iliasa, F.M. Photogrammetry as a Digital Tool for Joining Heritage Documentation in Architectural Education and Professional Practice. *Buildings* **2023**, *13*, 319. [CrossRef]
42. Abate, D. Built-Heritage Multi-Temporal Monitoring through Photogrammetry and 2D/3D Change Detection Algorithms. *Stud. Conserv.* **2019**, *64*, 423–434. [CrossRef]
43. Napolitano, R.; Glisic, B. Methodology for Diagnosing Crack Patterns in Masonry Structures Using Photogrammetry and Distinct Element Modeling. *Eng. Struct.* **2019**, *181*, 519–528. [CrossRef]
44. Galantucci, R.A.; Fatiguso, F. Advanced Damage Detection Techniques in Historical Buildings Using Digital Photogrammetry and 3D Surface Anlysis. *J. Cult. Herit.* **2019**, *36*, 51–62. [CrossRef]
45. Brumana, R.; Oreni, D.; Cuca, B.; Binda, L.; Condoleo, P.; Triggiani, M. Strategy for Integrated Surveying Techniques Finalized to Interpretive Models in a Byzantine Church, Mesopotam, Albania. *Int. J. Archit. Herit.* **2014**, *8*, 886–924. [CrossRef]
46. Lezzerini, M.; Antonelli, F.; Columbu, S.; Gadducci, R.; Marradi, A.; Miriello, D.; Parodi, L.; Secchiari, L.; Lazzeri, A. Cultural Heritage Documentation and Conservation: Three-Dimensional (3D) Laser Scanning and Geographical Information System (GIS) Techniques for Thematic Mapping of Facade Stonework of St. Nicholas Church (Pisa, Italy). *Int. J. Archit. Herit.* **2016**, *10*, 9–19. [CrossRef]
47. Fioretti, G.; Acciani, A.; Buongiorno, R.; Catella, M.A.; Acquafredda, P. Photogrammetric Survey and 3D Model as Experimental Tool for Mapping of Polychrome Marbles in Artworks: The Case of Two Baroque Altars in Bari (Italy). *J. Archit. Conserv.* **2019**, *25*, 90–103. [CrossRef]
48. Fioretti, G.; Acquafredda, P.; Calò, S.; Cinelli, M.; Germanò, G.; Laera, A.; Moccia, A. Study and Conservation of the St. Nicola's Basilica Mosaics (Bari, Italy) by Photogrammetric Survey: Mapping of Polychrome Marbles, Decorative Patterns and Past Restorations. *Stud. Conserv.* **2020**, *65*, 160–171. [CrossRef]
49. Fioretti, G.; Campobasso, C.; Capotorto, S. Digital Photogrammetry as Tool for Mensiochronological Analysis: The Case of St. Maria Veterana Archaeological Site (Triggiano, Italy). *Digit. Appl. Archaeol. Cult. Herit.* **2020**, *19*, e00158. [CrossRef]
50. Lavermicocca, N. Fragmenta: La Chiesa Bizantina Di Palazzo Simi. In *Bari, Sotto la Città. Luoghi Della Memoria*; Depalo, M.R., Radina, F., Eds.; Mario Adda Editore: Bari, Italy, 2008; pp. 61–64.
51. Depalo, M.R.; Cioce, M. Sotto Strada Lamberti Rivive la Storia. In *Bari, Sotto la città. Luoghi Della Memoria*; Depalo, M.R., Radina, F., Eds.; Mario Adda Editore: Bari, Italy, 2008; pp. 53–60.
52. Pacilio, G. Via Lamberti. In *Archeologia di una Città. Bari Dalle Origine al X Secolo*; Andreassi, G., Radina, F., Eds.; Edipuglia: Bari, Italy, 1988; pp. 545–550.
53. Bertelli, G. Gli Affreschi Di Età Bizantina Provenienti Dall'area Di S. Teresa Dei Maschi. In *Bari, Sotto la Città. Luoghi Della Memoria*; Depalo, M.R., Radina, F., Eds.; Mario Adda Editore: Bari, Italy, 2008; pp. 65–70.
54. Menges, F. Spectragryph-Optical Spectroscopy Software. 2022. Available online: http://www.effemm2.de/spectragryph/ (accessed on 23 May 2023).

55. Cesareo, R.; Gigante, G.E.; Castellano, A.; Ridolfi, S. Portable and Handheld Systems for Energy-Dispersive X-Ray Fluorescence Analysis. In *Encyclopedia of Analytical Chemistry*; Meyers, R.A., Ed.; John Wiley & Sons, Ltd.: Chichester, UK, 2009; p. a6803.pub2. [CrossRef]
56. Demirsar Arli, B.; Simsek Franci, G.; Kaya, S.; Arli, H.; Colomban, P. Portable X-Ray Fluorescence (p-XRF) Uncertainty Estimation for Glazed Ceramic Analysis: Case of Iznik Tiles. *Heritage* **2020**, *3*, 1302–1329. [CrossRef]
57. Elias, M.; Chartier, C.; Prévot, G.; Garay, H.; Vignaud, C. The Colour of Ochres Explained by Their Composition. *Mater. Sci. Eng. B* **2006**, *127*, 70–80. [CrossRef]
58. Mastrotheodoros, G.P.; Beltsios, K.G. Pigments—Iron-Based Red, Yellow, and Brown Ochres. *Archaeol. Anthr. Sci.* **2022**, *14*, 35. [CrossRef]
59. Mastrotheodoros, G.; Beltsios, K.G.; Zacharias, N. Assessment of the Production of Antiquity Pigments through Experimental Treatment of Ochres and Other Iron Based Precursors. *Mediterr. Archaeol. Archaeom.* **2010**, *10*, 37–59.
60. Daniel, F.; Mounier, A. Mobile Hyperspectral Imaging for the Non-Invasive Study of a Mural Painting in the Belves Castle (France, 15th C). *Sci. Technol. Archaeol. Res.* **2015**, *1*, 81–88. [CrossRef]
61. Tomasini, E.; Siracusano, G.; Maier, M.S. Spectroscopic, Morphological and Chemical Characterization of Historic Pigments Based on Carbon. Paths for the Identification of an Artistic Pigment. *Microchem. J.* **2012**, *102*, 28–37. [CrossRef]
62. Hofmann, C.; Rabitsch, S.; Malissa, A.; Aceto, M.; Uhlir, K.; Griesser, M.; Calà, E.; Agostino, A.; Fenoglio, G. The Miniatures of the Vienna Genesis: Colour Identification and Painters' Palettes. In *The Vienna Genesis*; Hofmann, C., Ed.; Böhlau Verlag: Wien, Austria, 2020; pp. 201–246. [CrossRef]
63. Radpour, R.; Fischer, C.; Kakoulli, I. New Insight into Hellenistic and Roman Cypriot Wall Paintings: An Exploration of Artists' Materials, Production Technology, and Technical Style. *Arts* **2019**, *8*, 74. [CrossRef]
64. Hradil, D.; Grygar, T.; Hradilová, J.; Bezdička, P. Clay and Iron Oxide Pigments in the History of Painting. *Appl. Clay Sci.* **2003**, *22*, 223–236. [CrossRef]
65. Hein, A.; Karatasios, I.; Mourelatos, D. Byzantine Wall Paintings from Mani (Greece): Microanalytical Investigation of Pigments and Plasters. *Anal. Bioanal. Chem.* **2009**, *395*, 2061–2071. [CrossRef] [PubMed]
66. Demir, S.; Şerifaki, K.; Böke, H. Execution Technique and Pigment Characteristics of Byzantine Wall Paintings of Anaia Church in Western Anatolia. *J. Archaeol. Sci. Rep.* **2018**, *17*, 39–46. [CrossRef]
67. Daniilia, S.; Minopoulou, E.; Andrikopoulos, K.S.; Tsakalof, A.; Bairachtari, K. From Byzantine to Post-Byzantine Art: The Painting Technique of St Stephen's Wall Paintings at Meteora, Greece. *J. Archaeol. Sci.* **2008**, *35*, 2474–2485. [CrossRef]
68. Švarcová, S.; Hradil, D.; Hradilová, J.; Čermáková, Z. Pigments—Copper-Based Greens and Blues. *Archaeol. Anthr. Sci.* **2021**, *13*, 190. [CrossRef]
69. Elert, K.; Herrera, A.; Cardell, C. Pigment-Binder Interactions in Calcium-Based Tempera Paints. *Dye. Pigment.* **2018**, *148*, 236–248. [CrossRef]